2022-01-28

Received: 26 October 2021 | Revised: 1 January 2022 | Accepted: 2 January 2022

DOI: 10.1002/er.7657

RESEARCH ARTICLE

INTERNATIONAL JOURNAL OF ENERGY RESEARCH WILEY

An innovated method to monitor the health condition of the thermoelectric cooling system using nanocomposite-based CNTs

Mohammed Al-Bahrani[1,2,3] | **Hasan Shakir Majdi**[4] | **Azher M. Abed**[2] | **Alistair Cree**[1]

[1]School of Engineering, Computing and Mathematics, University of Plymouth, Plymouth, UK

[2]Air Conditioning and Refrigeration Techniques Engineering Department, Al-Mustaqbal University College, Babylon, Iraq

[3]Iraqi Ministry of Oil, Midland Refineries Company, Baghdad, Iraq

[4]Department of Chemical Engineering and Petroleum Industries, Al-Mustaqbal University College, Babylon, Iraq

Correspondence
Mohammed Al-Bahrani, School of Engineering, Computing and Mathematics, University of Plymouth, Plymouth, PL4 8AA, UK.
Email: mohammed.naeem@plymouth.ac.uk; mohammed.naeem@mustaqbal-college.edu.iq

Summary

Many crucial applications use the thermoelectric coolers (TECs) system because they have some desirable properties, including durability, reliability, simple structure, and quietness. However, the performance of TECs is sensitive to any form of change and needs to be monitored constantly to ensure that they are working at their optimal. This paper proposes a novel approach for condition monitoring. This novel approach, unlike other attempts, does not need additional sensors but is directly carried out through the exploitation of the multi-wall carbon nanotubes (MWCNTs) piezoresistive property. For the suggested approach, a polyurethane (PU) resin was altered using various MWCNTs concentrations with the aim of constructing self-sensing nanocomposites sensors whose electrical conductivity is high. To investigate the electrical properties and microstructure of the constructed sensor, electrical resistance measurement, and scanning electron microscopy were used. From the results, it can be concluded that as the thickness increased, conductivity exhibited a monotonic increase. The peak electrical conductivity was 2.55 S. cm^{-1} for the 3.1 mm-thick MWCNTs sensors. This is approximately 5.1 above that of the 0.6 mm-thick MWCNTs sensors. Added to this, the MWCNT/PU sensors exhibited a high-temperature sensitivity with a negative temperature coefficient of resistance. The normalised resistance obtained from the sensor with the uppermost MWCNTs concentration is lower in comparison to the sensors with lower concentrations of MWCNTs. Additionally, the TEC cooling temperature influence on the tunnelling distance between MWCNTs was analytically estimated. This study's numerical results indicate that there is a potential correlation between TEC cooling generated temperature and the variations noted in the tunnelling distance between MWCNTs with an explicit impact on

the general nanocomposite sensors changes in electric resistance when the TEC system is in service.

KEYWORDS

health monitoring, MWCNTs, Peltier effect, self-sensing nanocomposite, thermoelectric coolers (TECs)

1 | INTRODUCTION

Many applications, ranging from cryogenic temperature controllers popular in the biotechnology and electronic fields to a broad range of general-purpose consumer appliances, require cooling.[1] The main role of the cooling system is to ensure that the temperature of the structure of the device does not exceed the thresholds imposed to maintain efficiency and safety.[2] In the area of electronics, one of the innovative cooling technologies is the thermoelectric coolers (TECs) system. This system employs an advanced technology thataccomplishes cooling based on the thermoelectric phenomena in various systems, including computers.[3] To work, this system relies on the Peltier effect. The Peltier effect results from the current as it passes through two different kinds of semiconductor metals.[4] The heat transfer by the current happens from one union to the next, and as one union cools, the next starts to heat up. In the event of a change in the current direction, the direction of the heat transfer also changes. This is the reason why Peltier cells sometimes play the role of heat pumps. The main advantage of the Peltier cell is that it is solid, produces no pollution, is extremely reliable, cools rapidly, and is small, among several other desirable characteristics.[5] Relative to the DC current input, the Peltier modules' performance can be defined as the optimal difference in temperature that can be attained between the module's surfaces (ΔTmax).

Several studies have focussed on evaluating the behaviour of the Peltier cell when used in cooling systems. From such studies, the different applications where Peltier cells and the materials used in making such cells can be noted.[6,7] For instance, Cosnier et al[8] conducted a numerical and experimental study of a thermoelectric air-cooling and air-heating system. The results from their study show that they attained a cooling power of 50 W per module, with a COP between 1.5 and 2. The researchers obtained these results by supplying an electrical intensity of 4 A and maintaining the temperature difference of 5°C between the hot and cool sides.

A numerical study was conducted by Wei He et al[9] exploring a thematic heating and cooling system powered by solar. When electrical power is applied to the device, it takes the role of a cooler. The lowest temperature attained is 17°C, and the thematic device's COP is above 0.24. A similar study by Shen et al[10] conducted an investigation of an innovative thermoelectric radiant air-conditioning system. Through reversing the input current, the system can both cool and heat indoor spaces using thermoelectric modules as radiant panels. After analysing a commercial thermoelectric module, the same scholars indicate that they achieved a peak cooling COP of 1.77, with the application of an electric current of 1.2, and sustaining a temperature of 20°C on the cold side. Chang et al[11] also studied an electric device's thermoelectric air-cooling module's performance. From the study, the scholars concluded that at a precise heat load, the thermoelectric cooling module attains the best cooling performance at a peak input current.

Studies have also noted that TECs have problems that can interfere with efficiency. For instance, the failure of a Peltier module results in the isolation of the cooled element from the cooler's heat sink. This results in the rapid deterioration of the stable temperature conditions of the element, which prompts the element to break down and isolate from the heating system. As a result of this, it becomes essential to come up with a monitoring method in the long term to help monitor the TECs health and performance. At the moment, there are a number of methods used in diagnosing the performance of TECs. The leading techniques for benchmarking TECs performance are software programs[12] and infrared thermal imager.[13] Mature as they are, these programs still face challenges in the areas of detecting the early stages of failure, tracking a systems degradation process when failure modes differ over time, and the methods assume that the semiconductor material's parameters as constant and temperature-dependent only. Moreover, the techniques require a high level of skills to use in the fault diagnosis process. Therefore, it has been suggested that evaluating Peltier module output parameters could produce misleading results.[14]

To deal with the challenges presented in the paragraph above, it has been suggested that the use of nanotechnology could deliver a potential solution for monitoring applications through manufacturing

nanocomposites, sometimes referred to as self-sensing nanocomposites. This could be achieved by the use of carbon nanotubes (CNTs) that take the role of multifunctional additive to the polymers to create a self-sensing nanocomposite.[15,16] Certain CNTs have superior thermal, electrical, and mechanical properties.[17,18] When incorporated as a nano-filler conductor into a resin matrix, even in small quantities, CNTs assist in the formation of electricity conductivity networks in the nanocomposite structure. Consequently, composites reinforced using CNT are commonly used in various applications like heating elements, temperature sensors,[19] electromagnetic applications,[20] pressure sensor,[21] strain sensor,[22] and in situ detection application.[23] Such nanocomposites are categorised under a kind of electrical resistor that is sensitive to temperature and has the capability to create thermal energy using electrical energy. For example, Blasdel et al[24] characterised a nanocomposite consisting of polypyrrole and multi-walled CNTs (MWCNTs), for temperature sensing. They concluded that the nanocomposite materials played the role of a sensor detector based on resistance change that was linearly proportional to the change in temperature.

As far as the author of this paper is concerned, there have not been any studies exploring the topic of monitoring the TEC system's health condition (ie, by evaluating the Peltier module output) using a new technique such as employed self-sensing nanocomposite materials for this purpose. Consequently, the present study introduces CNT reinforced composites as a smart nanocomposite sensor that can be applied to TEC for simultaneous monitoring to detect the produced Peltier temperature. A sonication method was employed for fabricating CNT-reinforced polymer composites with varying film thicknesses and CNT concentrations. This was followed by an investigation into the impact of the CNT concentration and film thickness on both temperature sensitivity and electrical conductivity. From the results, it can be concluded that reinforced polymer composites can serve as a potential smart nanocomposite material for determining the TECs health condition by monitoring its changes in temperature.

2 | EXPERIMENTAL PROCEDURE

2.1 | Materials

The purity of the filler material used for CNT/polyurethane (PU) nanocomposite was high (>95.0 wt%). The US Research Nanomaterials Inc. (Houston, TX, USA) provided the chemical vapour deposition grown MWCNTs. The MWCNTs had an average tube length and diameter of 60 μm and 5 to 10 nm, respectively. EasyComposites (Staffordshire, UK) supplied high purity acetone (>95%) and soft, flexible PU. The PU parts were mixed at a ratio of 1:1 by weight. The PU's viscosity was 450 mPa.s, with a characteristic demould period of one full day at 25°C. Nonetheless, a full cure would only be reached in another 7 days.

2.2 | MWCNT/PU nanocomposites manufacturing

To fabricate the MWCNTs/PU nanocomposites, the MWCNTs were dispersed uniformly in the PU matrix. Initially, numerous of the MWCNTs (0 → 2.5 wt%) concentrations were weighed and mixed in 70 mL of acetone in a glass beaker. To attain a uniform and full dispersion of the MWCNTs in the PU resin, a high frequency and intensity horn-type ultrasonicator (BR-20MT-10 L, 1000 W) was used. This method was employed with the aim of dealing with the Waals forces existing between the MWCNTs, which often results in the clumping together. With the aim of minimising any overheating effect, the ultrasonicator operated in an ice bath in the pulsed mode (intervals of 40 seconds on and 20 seconds off) for 20 minutes. Once the MWCNTs had been sonicated, a precise quantity of PU raising was amalgamated into the mixture. The ultrasonicator was then used to disperse the mixture for an extra 4 minutes. Once fully dispersed, the mixture was then put in an oven at 60°C for 24 hours so that the acetone could be allowed to evaporate. With the evaporation complete, a hardener was introduced using a mix ratio of 1:1 and mixed thoroughly for another 4 minutes. This was followed by a degassing of the mixture in a vacuum chamber for 20 minutes to get rid of any undesirable air bubbles. To get the specimen configuration required for testing, the mixture was then cast in a mould (with varying thicknesses). The final process involved curing the mixture at 30°C for 24 hours and then for another 7 days a room temperature to ensure that the curing process was complete.

2.3 | Characterisation

For evaluating the MWCNTs in the matrix dispersion degree, light transmitted optical microscopy (TOM) was used to observe non-cured MWCNTs/PU mixtures without the hardener and before the curing phase. Binocular microscope Axiolab 5, supplied by Appleton Woods Limited, United Kingdom, was used. A high resistance digital multimeter (Keithley 2100) was used to assess the prepared nanocomposite specimens' electrical conductivity.

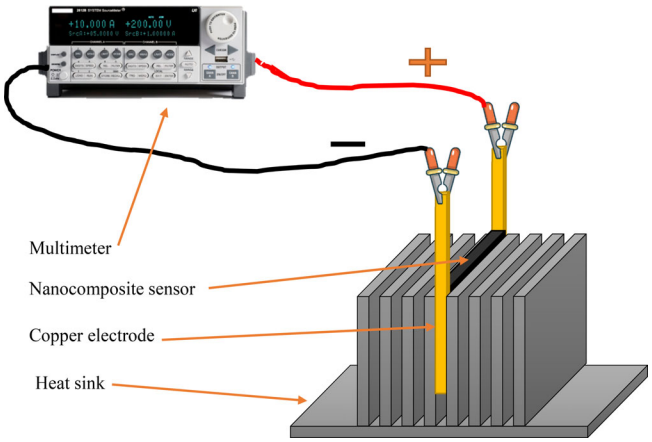

FIGURE 1 Schematic layout of the MWCNTs/PU nanocomposite sensor placed between the heat sink fins

Using this method made it possible to measure the samples' electric resistance. To deal with any errors that could emanate from the contact resistance at the test probe's tip and the surface, high purity silver paint was applied to the specimens to take the role of electrode sites. Equation (1) can be used to calculate the sample's electrical conductivity:

$$\sigma = \frac{L}{RA}, \tag{1}$$

where R represents the sample's electrical resistance (Ω), A and L stand for the cross-sectional area (cm^2), and the samples' respective lengths (cm). The change in resistance of MWCNTs/PU sensor under temperature was monitored to accomplish temperature sensing. As can be seen in Figure 1, the MWCNTs/PU nanocomposite sensors were put in the heat sink (ie, between the fins). The multimeter then simultaneously recorded the change in resistance for multiple MWCNTs/PU sensors thickness.

Using the external heat system and the Peltier TEC, a mini thermoelectric system was constructed as shown in Figure 2. Typically, the module's specification can be obtained from the supplier, as can be seen in Table 1. The installation began with the electronic module (ie, Peltier) located between the heat sinks. This was followed by the installation of the cooling fan in the heat sink. The installation of the heat sinks had the aim of enhancing the heat rejection effect. The Peltier cell was placed (ie, sandwiched) between heat sinks and cooler fans. To join each of them, thermal paste and screws were used. The power supply for the system was 12 V and 6 A. Following the switching on of the power, the internal space temperature and cooling temperature (T_c) were measured. The ambient temperature was also recorded because the experiment process was done in an open environment condition. The data for the temperature measurement was logged at one-minute intervals. The experiment was done for an hour with the aim of getting a steady drop in temperature in the thermoelectric cooling system.

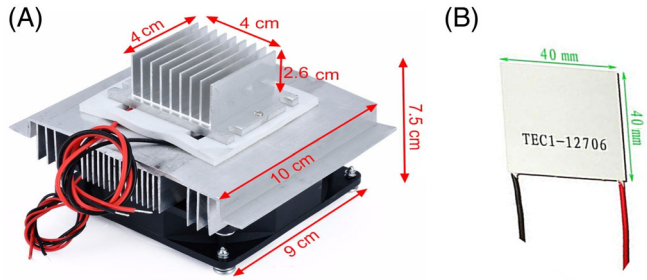

FIGURE 2 (A) Installation of the Peltier module with the heat sinks and cooler fans and (B) TEC 12706 Peltier module

TABLE 1 Peltier module characteristics

Peltier model (TEC 12706)	Characterisation
Maximum voltage, Vmax	12 V
Maximum current, Imax	6 Ampere
Maximum temperature difference, (ΔT) max	68°C
Maximum power consumption, Qmax	60 W
Electrical resistivity (ρ)	1.2×10^{-2} Ωcm
Seebeck coefficient (α)	2.2×10^{-4} V/K
Thermal conductivity (k)	1.62×10^{-2} W/cmK

3 | RESULTS AND DISCUSSION

3.1 | Sensor electrical conductivity

In Figure 3, the MWCNTs/PU nanocomposites sensor's electrical conductivity measurements are illustrated as a function of weight % MWCNTs concentration. From that illustration, it becomes clear that there is a considerable increase from 0.0 to 0.5 wt% of MWCNTs. Thus, the change in conductivity observed, up to 2.5 wt% MWCNTs, was gradual. In the present study, the percolation threshold, which denotes the lowest weight % MWCNT content in the matrix, after which there is no considerable change in the recorded electrical conductivity. It can also be noted that in the present study, the highest MWCNTs/PU nanocomposite sensor electric conductivity attained was 3.25×10^{-2} S/cm, at 2.5 wt% MWCNTs. The recorded escalation in nanocomposite conductivity could most probably be a result of a

well-constructed MWCNTs network arrangement (conducting pathways) established using a matrix material.[25,26] The homogenous character of the MWCNTs distribution in the matrix material in comparison to unmodified PU is illustrated in Figure 4. When MWCNTs are in low concentration, there is a considerably large distance between neighbouring MWCNTs. The distance becomes smaller with the increase of the concentration. This results in the electronic transfer effectiveness (ie, transfer of electrons) between the MWCNTs being extremely reliant on this MWCNTs spacing distance. The ease with which the transfer of electrons happens at higher concentrations is thought to be augmented by the mechanism for tunneling. However, there is a high possibility that carbon tubes will agglomerate if the MWCNTs concentration exceeds 2.5 wt%. The agglomeration of CNTs will lead to a decrease in the activity of the CNTs surface area characteristics and then minimise the mechanical and electrical properties of the nanocomposite.[16] Moreover, the electrical properties of the nanocomposite are highly dependent on the MWCNTs dispersion and concentration. Agglomerates of MWCNTs will cause abnormality in the conductive network, which will minimise the effect of the piezo-resistivity property of the nanocomposite.[27] On the basis of the results of the present study, high electrical

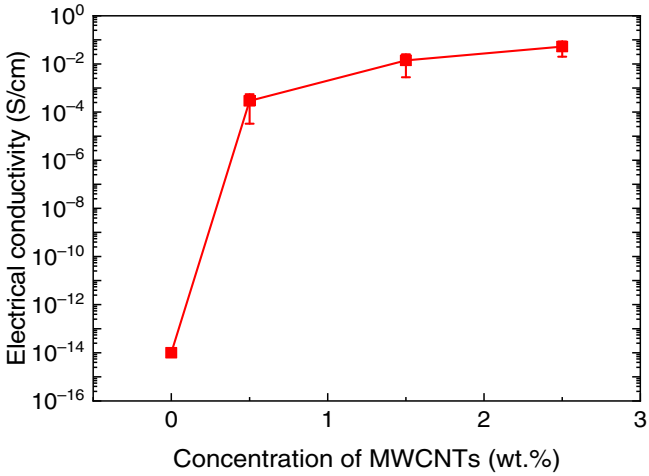

FIGURE 3 Electrical conductivity of MWCNTs/PU nanocomposite sensors as a function of MWCNTs concentrations

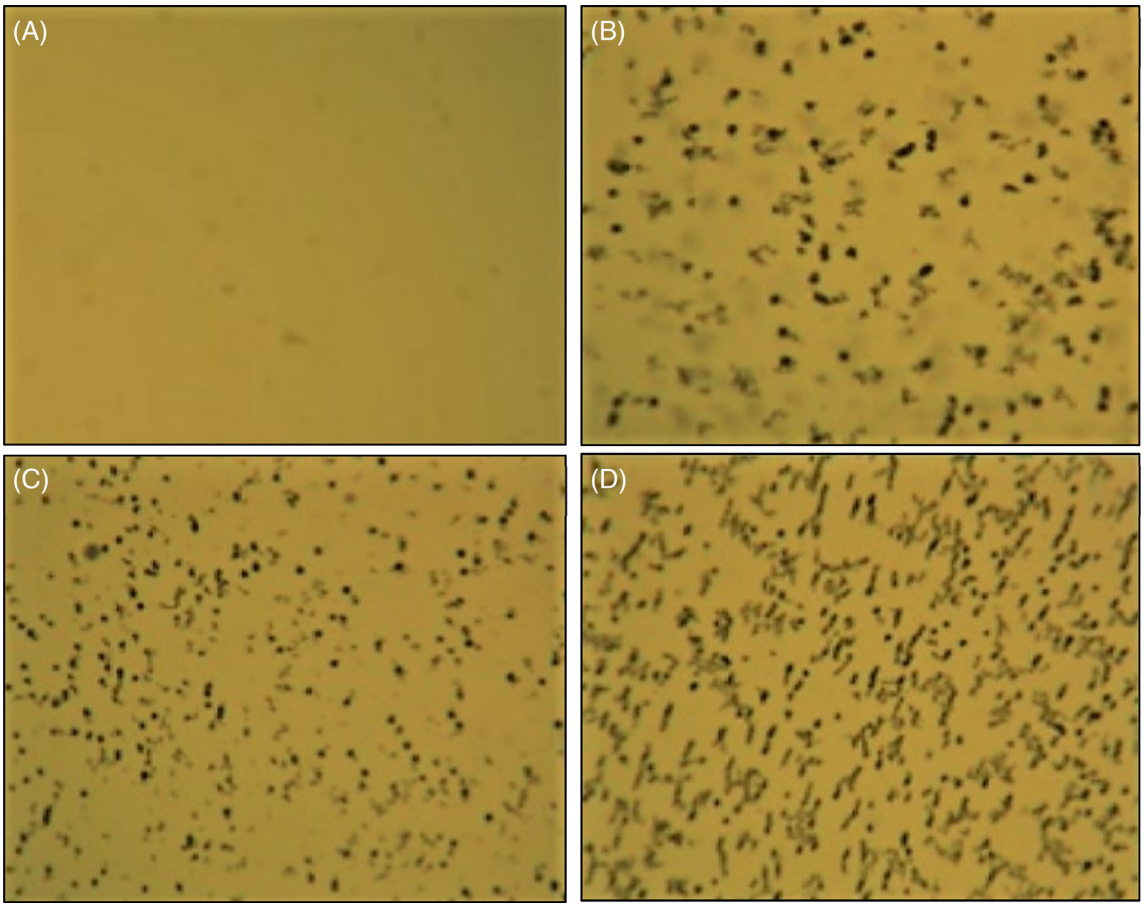

FIGURE 4 TOM images of the MWCNTs/PU with different MWCNTs concentrations (A) 0, (B) 0.5, (C) 1.5, and (D) 2.5 wt% MWCNTs content

conductivity was noted from the nanocomposite sensor, at 2.5 wt% of MWCNTs. Hence, the concentration of MWCNTs was sustained at 2.5 wt% for the experiments that followed.

3.2 | Impact of sensor thickness on electrical conductivity

Nanocomposite sensors with varying thicknesses of 2.5 wt% of CNTs were prepared using layer-by-layer fabrication with the aim of determining the influence of sensor thickness on the electrical property (ie, resistance conductivity). The MWCNTs/PU nanocomposite sensors' relativity change as a function of thickness is presented in Figure 5. As anticipated, the sensors' resistance decreased considerably with the increase in the thickness of MWCNTs/PU nanocomposite sensors. Equation (1) was used to calculate the sensor's electric conductivity and its various thicknesses. Results show that there was a monotonic increase in electronic conductivity as thickness also increased. The peak electrical conductivity was 0.55 $S.m^{-1}$ for the 3.1 mm-thick MWCNTs sensors. This represents 5.1 times above the MWCNTs sensor, which is 0.6 mm thick. The MWCNTs sensor's electrical conductivity is primarily determined by the conducting channels' density in a random MCWNTs network, which is anticipated to be proportional to the low-resistance inter-tube junctions' concentration formed by MWCNTs.[28] Regulating the layer-by-layer fabrication thickness was done with the anticipation that an increase in thickness could result in a higher density of the MWCNTs networks, which will result in an escalation of the MWCNTs/PU sensors' electrical conductivity. Using the results above as a basis, the 0.6 and 3.1 mm-thick MWCNTs/PU sensors' performance will be considered in any future experiments because the electrical conductivities of both samples are different.

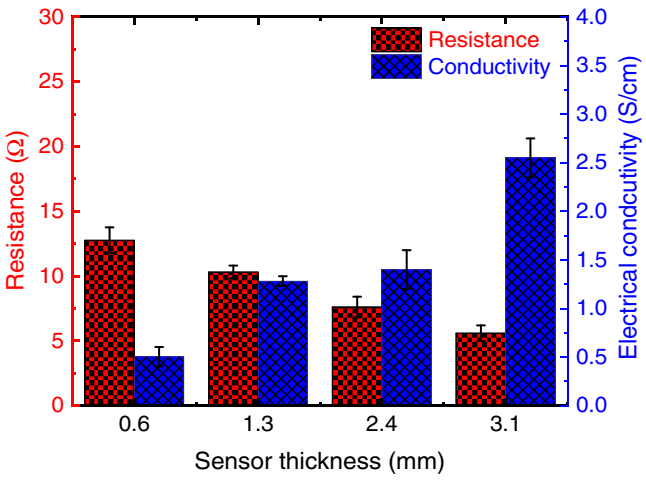

FIGURE 5 Electrical conductivity and resistance change of MWCNTs/PU nanocomposite sensors with varied thicknesses

3.3 | TEC cooling temperature status monitoring

If a TEC is connected to a supply of power, the current starts flowing across the junction between two main wires of the TEC. This results in heat transfer from one TEC surface side to another because of the Peltier effect. Because of the sudden drop in TEC surface temperature, the cooler's heat is transmitted to the hot surface from the cold surface. As illustrated in Figure 6A, the cold temperature dropped below the ambient temperature. Ahead of attaining a stable state temperature, the surface temperature of the TEC dropped to its lowest level of 15°C before settling into a stable state at around 12.5°C for more than 3 hours. As a way of monitoring this behaviour, Figure 6B shows the MWCNT/PU nanocomposite sensors' resistance change at varying temperatures and thicknesses (cooling side) when the TEC is left on for more than 3 hours. The developed MWCNTs/PU nanocomposite sensors' resistance increased as the TEC temperature lowered, indicating a negative temperature coefficient (NTC).

The concept of NTC stipulates that materials' resistance escalates with lowering the temperature and vice versa.[29] The development of a flocculated conductive structure under various temperatures is the cause of the NTC effect.[30] Also, the change, over a period, in the sample's normalised resistance is smaller in comparison to the low MWCNTs (ie, 0.6 mm-thick). In comparison to the lower MWCNTs concentration, the MWCNTs/PU sensor with higher concentrations of CNT indicated lower noise levels. Such behaviour could be linked to the MWCNTs network structure's better stability, which is connected to the higher MWCNTs concentrations that boost electronic transfer via inter-particle channels.[31] On this basis, the MWCNTs/PU sensors' NTC can play the role of metric monitoring for the cooling temperature status when TEC is working.

3.4 | Sensor stability and reliability

Reliability, which denotes stability in the operation of any method being developed, is a requirement if such a method is to be accepted. For this reason, in the present study, this method's stability was analysed as a function of time through iterating the system at work (ie, switching it on and off at 3-minute

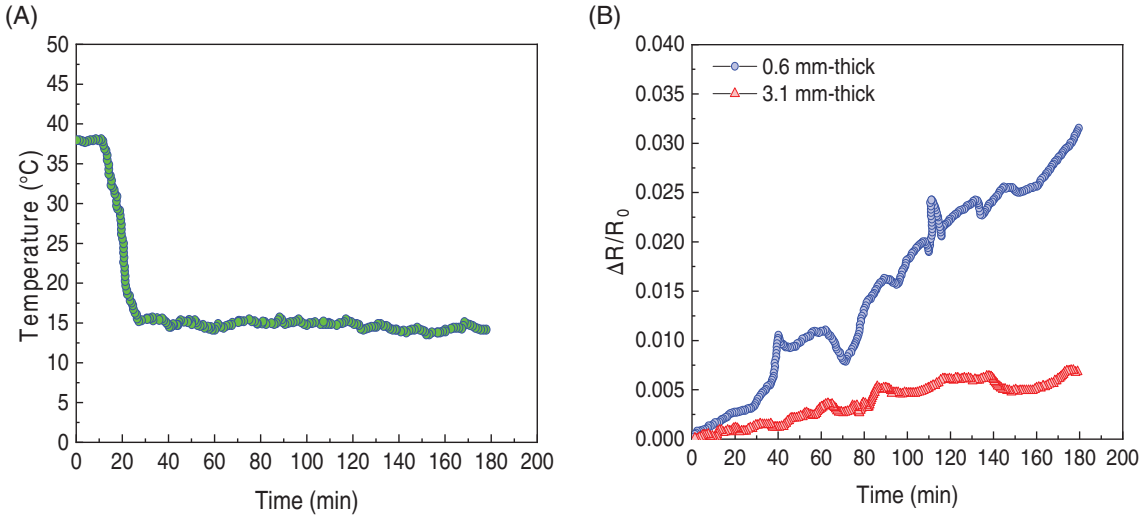

FIGURE 6 (A) TEC cold temperature vs time and (B) normalised resistance vs time of MWCNTs/PU nanocomposite sensors with varied thicknesses during TEC working

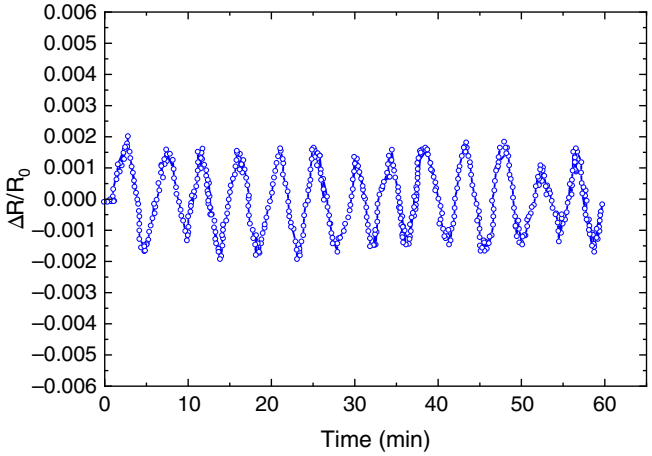

FIGURE 7 Change in normalised resistance ($\triangle R/R_0$) as a function of time during TEC system working (on/off) as a cyclic test for nanocomposites sensor filled with 2.5 wt% of MWCNTs concentrations

intervals) on the same specimen. Figure 7 presents the cyclic test effect on the electrical resistance changes of the self-sensing nanocomposite specimens with 2.5 wt% MWCNTs concentrations. Also, it can be seen that the resistance changes values ($\triangle R/R_0$) escalate steadily as time also increases when the TEC system is switched on and then starts to decrease gradually when the system is switched off, showing an excellent correspondence tendency. There are two potential phenomena that happened during the cyclic test that can be used to explain this. The first is the demolition of the prevailing MWCNTs conductive networks and then the construction of new MWCNTs conductive contacts.

When the cooling temperature affected the sensor, the motion of the polymer molecules also affected the conductive MWCNTs networks. This resulted in the escalation of gaps between the neighbouring MWCNTs, leading to an increase in the value of the $\Delta R/R_0$. The second explanation is that once the temperature starts to increase as a result of the TEC system being switched off, the $\Delta R/R_0$ values also decrease because of the tunnelling gaps between the MWCNTs, which became narrower so that the electrons could have easy passage between the MWCNTs.[32,33]

3.5 | The sensor's in situ mechanism

The MWCNTs/PU sensor with a higher concentration of MWCNTs (ie, high thickness) exhibited lower noise levels in comparison to the one with the lower concentration of MWCNTs. This is the basis on which it is used in the present study for the investigation of the sensor mechanism. It has been shown that when the dispersion of MWCNTs in polymeric resin materials is good, these materials have a higher capability to pathways that are highly electrically conductive. Such uninterrupted conductive pathway networks in nanocomposites, which are a result of excellent MWCNTs contact, can transmit electrical current and are an effective electrical pathway for the nanocomposite systems.[34] In this mechanism, the sensor's MWCNTs network alters following the sensor's exposure to the cooling temperature generated in the TEC system. Before the application of the temperature to the sensor, the MWCNTs conductive network's positions and distribution enjoyed a high level of stability with a constant distance between all neighbouring MWCNT-

MWCNT conductive networks. Once the temperature was applied to the sensor, the MWCNTs became stretched and wriggled with the PU molecular chains. This resulted in the breaking of the MWCNTs conductive pathways and an intensification of the tunnelling gaps between MWCNTs. Considering that the distribution of MWCNTs inside the sensor matrix is random, the calculation of the distance between every two neighbouring MWCNTs can be accomplished through Simon's theoretical model.[35] This is expressed as;

$$R_{\text{tunnel}} = \frac{h^2[d]}{Ae^2\sqrt{2m\beta}}\exp\left(\frac{4\pi[d]}{h}\sqrt{2m\beta}\right), \tag{2}$$

where d represents the space between adjacent MWCNTs, e the electron electric charge density ($=1.60217662 \times 10^{-19}$ coulombs), m the electron mass ($= 9.10938356 \times 10^{-31}$ kg), h the Plank's constant ($=6.62607004 \times 10^{-34}$ m^2 kg/s), and A is cross-sectional tunnel area (the cross-sectional area of CNT is approximately used here). β denotes the energy barrier (0.5-5 eV) for the majority of polymers in the present study; β used 2.5 eV.[36] Further, the electrical resistance of the sensor after being exposed to temperature (R_2) can be assumed using;

$$R_2 = R_0 + \Delta R_{\text{tunneling}}, \tag{3}$$

where R_0 stands for the specimen's resistance before being exposed to temperature and $\Delta R_{\text{tunnelling}}$ denotes resistance to change (after the temperature was applied) for the tunnelling distance between MWCNT-MWCNT. In a similar manner, after the sensor was impacted by the temperature, the distance between neighbouring MWCNTs changed because the MWCNTs network had been damaged. Consequently, tunnelling resistance can be assumed using:

$$\Delta R_{\text{tunnel}} = \frac{h^2[\Delta d]}{Ae^2\sqrt{2m\beta}}\exp\left(\frac{4\pi[\Delta d]}{h}\sqrt{2m\beta}\right). \tag{4}$$

From Equation (4), it becomes clear that the tunnelling resistance is intensely reliant on both the tunnelling distance (ie, d) and the energy barrier of the matrix (e). Therefore, combining Equation (3) and (4) results in;

$$\frac{(R_2 - R_0)}{R_0} = \frac{\Delta R}{R_0} = \left(1 + \frac{h^2[\Delta d]}{Ae^2\sqrt{2m\beta}}\exp\left(\frac{4\pi[\Delta d]}{h}\sqrt{2m\beta}\right)\right)/R_0. \tag{5}$$

Furthermore, the connection between sensor resistance and temperature (generated from the TEC) was scrutinised. Figure 6 shows the results of this investigation. As can be noted from the results, the sample's resistance lowers as the temperature increases, making it possible to characterise the NTC thermistor. Resistance of the NTC thermistor can be characterised following the fitting of the curve, as can be seen in Figure 8.

$$\frac{\Delta R}{R_0} = 5.04471 \times \exp^{(-T_c/1.7116)} + 0.00477 \times \exp^{(-T_c/31.45173)} - 6.45049 \times 10^{-4}, \tag{6}$$

where T_C stands for the cooling temperature generated from the TEC system. Therefore, combining Equation (5) with Equation (6) results in

$$3.934700717 \times 10^9 \times e^{(-0.5842486562 \times T_C)} + 3.720436342 \times 10^6 \times e^{(-0.03179475342 \times T_C)} - 8.302734772 \times 10^6 = d \times \sqrt{2} \times e^{(2.861991506 \times 10^{19} \times d)} \tag{7}$$

Based on the natural logarithm of both sides of Equation (7) and from the value of T_C obtained, the space between adjacent MWCNTs (d) can be calculated using the following formulas:

$$T_C = -1.623262232 \times \ln(d) - 6.504067807 \times 10^{19} \times d + 33.99725207. \tag{8}$$

The term on the top right-hand side of Equation (7) describes the generation of the cooling temperature from

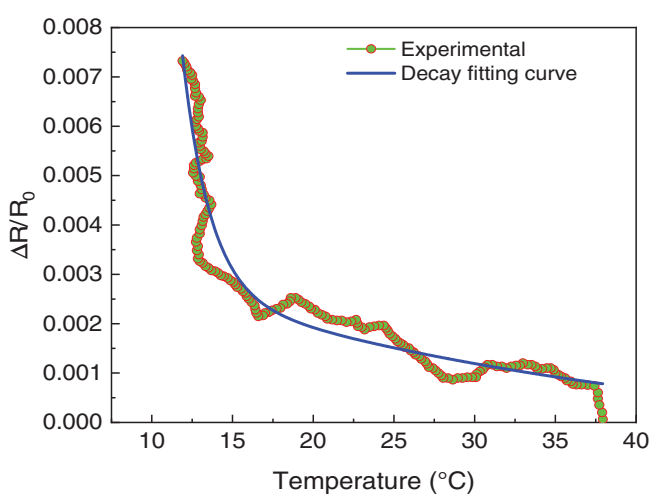

FIGURE 8 Plot of normalised change in resistance as a function of temperature. The solid line is the decay fitting curve, while the solid circles are experimental results

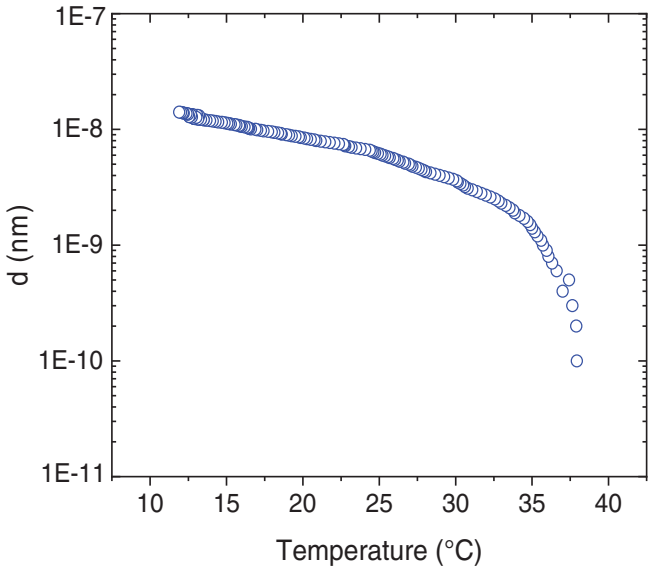

FIGURE 9 Plot of tunnelling distance (d) of MWCNTs/PU nanocomposite sensor as a function of the TEC cooling temperature

the TEC system. The second and third terms on Equation (2) "s right-hand side provide the tunnelling distance between the sensors" MWCNT-MWCNT. All the equations provide a description of the connection between the distance between every two neighbouring MWCNTs and the temperature variation. Figure 9 presents the numerical results obtained from the use of Equation (8). From the results, it is clear that the tunnelling distance decreases significantly in a nonlinear fashion as the cooling temperature increases. This can be credited to the fact that the nanocomposite sensor prepared exhibited a NTC trend. This behaviour can be explained by noting that an increase in temperature leads to a reduction in the gap between MWCNT and MWCNT as the PU resin chains decrease.[37]

4 | CONCLUSION

It can now be concluded that self-sensing nanocomposites were fabricated with the aim of using them as a simple mechanism for monitoring the TEC system's health condition. As a result of the uniform dispersion of MWCNTs in the PU matrix, a boost in electrical conductivity was attained. It was noted that the electrical conductivity increased by a number of orders after MWCNTs were introduced. The highest value ($\approx 3.25 \times 10^{-2}$ S.cm^{-1}) was at 2.5 wt% of MWCNTs concentration. As the thickness increases, the electrical conductivity also shows a monotonic increase. For the 3.1 mm-thick MWCNTs sensors, the peak electrical conductivity was 2.55 S.cm^{-1}, higher when compared to the MWCNTs sensor's 0.6 mm. Regarding monitoring the system's behaviour, the developed MWCNTs/PU nanocomposite sensors increased as The TEC temperature decreased, exhibiting a NTC trend. Also, with time, the normalised resistance of the sample with the highest concentration of MWCNTs is smaller in comparison to the samples with lower concentrations of MWCNTs. Furthermore, the MWCNTs/PU sensor with a higher CNT concentration produced lower levels of noise in comparison to sensors with lower concentrations. When put through multi-cyclic testing, the nanocomposite sensor was investigated to test the sensor's reliability. From the testing, the results indicate excellent correspondence behaviour when the TEC system is subjected to the on/off mode. The numerical results obtained in this study provide a clear indication of the efficiency of the kind of sensor under study. They show that there is a considerable nonlinear decrease in tunnelling distance with every increase in TEC cooling temperature. Therefore, it is posited that in situ, real-time, and electrical resistance measurement in the developed self-sensing composite materials deliver possibilities for an online technique for sensing and assessing the TEC system's health condition, which lowers the potential for an unexpected disastrous failure happening. Finally, to make the initial finding of this study more general. Therefore, for future work, it is also necessary to use other filler such as Graphene and carbon nanofibers for monitoring applications due to their superior properties.

ACKNOWLEDGEMENTS

The authors would like to thank the Iraqi ministry of oil and Al-Mustaqbal University College to support this study. The authors appreciate the support of school of engineering staff and laboratories at the University of Plymouth to carry out some of the required tests.

ORCID

Mohammed Al-Bahrani https://orcid.org/0000-0003-0680-0116

REFERENCES

1. Tohidi F, Holagh SG, Chitsaz A. Thermoelectric generators: a comprehensive review of characteristics and applications. *Appl Therm Eng*. 2022;201:117793.
2. Jouhara H, Żabnieńska-Góra A, Khordehgah N, et al. Thermoelectric generator (TEG) technologies and applications. *Int J Thermofluids*. 2021;9:100063.
3. Putra N, Iskandar FN. Application of nanofluids to a heat pipe liquid-block and the thermoelectric cooling of electronic equipment. *Exp Thermal Fluid Sci*. 2011;35:1274-1281.
4. Zhao D, Tan G. A review of thermoelectric cooling: materials, modeling and applications. *Appl Therm Eng*. 2014;66:15-24.

5. Sharma S, Dwivedi V, Pandit S. A review of thermoelectric devices for cooling applications. *Int J Green Energy*. 2014;11:899-909.
6. Twaha S, Zhu J, Yan Y, Li B. A comprehensive review of thermoelectric technology: materials, applications, modelling and performance improvement. *Renew Sust Energ Rev*. 2016;65:698-726.
7. Elsheikh MH, Shnawah DA, Sabri MFM, et al. A review on thermoelectric renewable energy: principle parameters that affect their performance. *Renew Sust Energ Rev*. 2014;30:337-355.
8. Cosnier M, Fraisse G, Luo L. An experimental and numerical study of a thermoelectric air-cooling and air-heating system. *Int J Refrig*. 2008;31:1051-1062.
9. He W, Zhou J, Hou J, Chen C, Ji J. Theoretical and experimental investigation on a thermoelectric cooling and heating system driven by solar. *Appl Energy*. 2013;107:89-97.
10. Shen L, Xiao F, Chen H, Wang S. Investigation of a novel thermoelectric radiant air-conditioning system. *Energ Buildings*. 2013;59:123-132.
11. Chang Y-W, Chang C-C, Ke M-T, Chen S-L. Thermoelectric air-cooling module for electronic devices. *Appl Therm Eng*. 2009;29:2731-2737.
12. Cotfas PA, Cotfas DT. Comprehensive review of methods and instruments for photovoltaic–thermoelectric generator hybrid system characterization. *Energies*. 2020;13:6045.
13. Wang Y, Shi Y, Liu D. Performance analysis and experimental study on thermoelectric cooling system coupling with heat pipe. *Procedia Eng*. 2017;205:871-878.
14. Ahiska R, Ahiska K. New method for investigation of parameters of real thermoelectric modules. *Energy Convers Manag*. 2010;51:338-345.
15. Al-Bahrani M, Cree A. Micro-scale damage sensing in self-sensing nanocomposite material based CNTs. *Compos Part B*. 2021;205:108479.
16. Al-Bahrani M, Bouaissi A, Cree A. Mechanical and electrical behaviors of self-sensing nanocomposite-based MWCNTs material when subjected to twist shear load. *Mech Adv Mater Struct*. 2021;28:1488-1497.
17. De Volder MFL, Tawfick SH, Baughman RH, Hart AJ. Carbon nanotubes: present and future commercial applications. *Science*. 2013;339:535-539.
18. Bedsole RW, Park C, Bogert PB, Tippur HV. A critical evaluation of the enhancement of mechanical properties of epoxy modified using CNTs. *Mater Res Exp*. 2015;2:095020.
19. Neitzert HC, Vertuccio L, Sorrentino A. Epoxy/MWCNT composite as temperature sensor and electrical heating element. *IEEE Trans Nanotechnol*. 2010;10:688-693.
20. Yusof Y, Moosavi S, Johan MR, et al. Electromagnetic characterization of a multiwalled carbon nanotubes–silver nanoparticles-reinforced polyvinyl alcohol hybrid nanocomposite in X-band frequency. *ACS Omega*. 2021;6:4184-4191.
21. Kanoun O, Bouhamed A, Ramalingame R, Bautista-Quijano JR, Rajendran D, Al-Hamry A. Review on conductive polymer/CNTs nanocomposites based flexible and stretchable strain and pressure sensors. *Sensors*. 2021;21:341.
22. He Y, Wu D, Zhou M, et al. Wearable strain sensors based on a porous polydimethylsiloxane hybrid with carbon nanotubes and graphene. *ACS Appl Mater Interfaces*. 2021;13:15572–15583.
23. Al-Bahrani M, Cree A. In situ detection of oil leakage by new self-sensing nanocomposite sensor containing MWCNTs. *Appl Nanosci*. 2021;11:2433-2445.
24. Blasdel NJ, Wujcik EK, Carletta JE, Lee K-S, Monty CN. Fabric nanocomposite resistance temperature detector. *IEEE Sensors J*. 2014;15:300-306.
25. Dinh NT, Kanoun O. Temperature-compensated force/pressure sensor based on multi-walled carbon nanotube epoxy composites. *Sensors*. 2015;15:11133–11150.
26. Shen JT, Buschhorn ST, De Hosson JTM, Schulte K, Fiedler B. Pressure and temperature induced electrical resistance change in nano-carbon/epoxy composites. *Compos Sci Technol*. 2015;115:1-8.
27. Reddy PN, Kavyateja BV, Jindal BB. Structural health monitoring methods, dispersion of fibers, micro and macro structural properties, sensing, and mechanical properties of self-sensing concrete—a review. *Struct Concr*. 2021;22:793-805.
28. Ventura IA, Zhou J, Lubineau G. Investigating the inter-tube conduction mechanism in polycarbonate nanocomposites prepared with conductive polymer-coated carbon nanotubes. *Nanoscale Res Lett*. 2015;10:1-5.
29. Cui M-M, Zhang X, Liu K-G, Li H-B, Gao M-M, Liang S. Fabrication of nano-grained negative temperature coefficient thermistors with high electrical stability. *Rare Metals*. 2021;40:1014-1019.
30. Xiang ZD, Chen T, Li ZM, Bian XC. Negative temperature coefficient of resistivity in lightweight conductive carbon nanotube/polymer composites. *Macromol Mater Eng*. 2009;294:91-95.
31. Al-Bahrani M, Graham-Jones J, Gombos Z, Al-Ani A, Cree A. High-efficient multifunctional self-heating nanocomposite-based MWCNTs for energy applications. *Int J Energy Res*. 2020;44:1113-1124.
32. Bao WS, Meguid SA, Zhu ZH, Weng GJ. Tunneling resistance and its effect on the electrical conductivity of carbon nanotube nanocomposites. *J Appl Phys*. 2012;111:93726.
33. Yu Y, Song G, Sun L. Determinant role of tunneling resistance in electrical conductivity of polymer composites reinforced by well dispersed carbon nanotubes. *J Appl Phys*. 2010;108:84319.
34. Li C, Thostenson ET, Chou TW. Effect of nanotube waviness on the electrical conductivity of carbon nanotube-based composites. *Compos Sci Technol*. 2008;68:1445-1452.
35. Perets Y, Aleksandrovych L, Melnychenko M, Lazarenko O, Vovchenko L, Matzui L. The electrical properties of hybrid composites based on multiwall carbon nanotubes with graphite nanoplatelets. *Nanoscale Res Lett*. 2017;12:406.
36. Hu N, Karube Y, Arai M, et al. Investigation on sensitivity of a polymer/carbon nanotube composite strain sensor. *Carbon*. 2010;48:680-687.
37. Chu K, Kim D, Sohn Y, Lee S, Moon C, Park S. Electrical and thermal properties of carbon-nanotube composite for flexible electric heating-unit applications. *IEEE Electron Dev Lett*. 2013;34:668-670.

How to cite this article: Al-Bahrani M, Majdi HS, Abed AM, Cree A. An innovated method to monitor the health condition of the thermoelectric cooling system using nanocomposite-based CNTs. *Int J Energy Res*. 2022;1-10. doi:10.1002/er.7657